Development of Radiographic Image Processing Algorithms at CNL

Krassimir STOEV [1]

[1] Canadian Nuclear Laboratories, Chalk River, Ontario K0J 1J0, Canada
Phone: +1-613-584-3311 extension 43970, Fax: +1-613-584-8110; e-mail: Krassimir.Stoev@CNL.ca

Abstract
Image processing software is an important tool during analysis and interpretation of digital radiography images. CNL is currently in the process of developing software, which will be used for implementation and testing of new image processing algorithms. The current state of the CNL image processing software is discussed. Basic functionality is described. Examples of currently implemented advanced image processing techniques are presented. Details of different bilateral filtering/smoothing algorithms are compared.

Keywords: radiography, image processing

1. Introduction

Digital radiography (DR) is a fast and reliable volumetric inspection and diagnostics method which can be used for testing of a variety of objects made from different materials. DR offers several advantages in comparison to classical film radiography, such as improved detector dynamic range (i.e., a wider range of material thickness can be radiographed simultaneously), improved productivity (due to higher sensitivity of the digital detectors significantly reducing exposure times), improved safety due to lower exposure levels, reduced costs of consumables, etc. As a result, DR allows for integration and automation of the data collection, storage, archiving and transmission processes, and offers improved information flow and data management. Image processing is very important to digital radiography, and allows for better interpretation of radiographs. CNL has developed a prototype image processing software, which is constantly being upgraded and improved. This software is used not only for processing of radiographic images, but also as a test bed for development and evaluation of new image processing algorithms [1].

2. Description of the software and implemented algorithms

In 2010, CNL started development of an image processing software (called CNL Image Processing Tool, or IPT), which was intended to be used for implementation and testing of new image processing algorithms. At the current stage, all basic editing and image manipulation functions are implemented [1], and work is underway on the development of advanced image processing algorithms and their implementation and testing. The main window of the software has three regions: menus, control buttons, and display area (see Figure 1). The IPT software is designed to work with 16-bit TIFF images, but can read and save other formats of images. The following basic image processing options are available in the menus and in the control buttons area: Selection Tool, Zoom (1% to 1000%, fit width, height, stretch, selection), Magnifying Glass Tool, Invert Image, Rotate, Flip Horizontally or Vertically, Crop Selection, Multiply, Intensity Filtering (i.e., Median, Average, Gaussian, Min/Max), Spatial Filters (Gradient, Laplacian, Sobel, Prewitt, Shift/Difference, Line Segment), Crop, Copy, Paste, Invert, Despeckle, Set or Stretch Brightness / Contrast / Gamma / Histogram Contrast, Line-Profile Tool, Histogram Display, Equalize Image Histogram, Unsharp Mask, Smoothing, Sharpen, Emboss. All of these options are basic image manipulation options, and can be used for initial assessment of the radiographic images.

Figure 1. Main window of IPT: menus (1), control buttons (2), and display area (3)

After implementing the basic image editing, manipulation and processing options, work was concentrated on the development of advanced image processing algorithms and their implementation. Several types of algorithms were developed and tested:

- Methods for image noise suppression (such as smoothing and differential operators based on fitting with orthogonal polynomials, bilateral smoothing filters, etc.).
- Methods for image contrast enhancement (such as local contrast enhancement techniques based on local signal variance, adaptive unsharp mask, adaptive contrast enhancement, FACOR filter, etc.).
- Methods for image grey-scale manipulation (such as pixel-based mathematical transformations, continuous linear unrestricted image intensity adjustment, non-linear continuous intensity remapping, global and local non-linear histogram equalization, adaptive histogram equalization (AHE), contrast-limited AHE (CLAHE), etc.).
- Methods for statistical image analysis (such as 16-bit line-profile, horizontal and vertical integrated line profile, image and area statistics, algorithm for removing outlier values, etc.).
- Methods based on two-dimensional Fast Fourier Transform (FFT)
- Methods based on two-dimensional Discrete Wavelet Transform (DWT)

Some of these methods will be discussed in detail in the following sections.

2.1 Noise suppression methods

Noise suppression, also called smoothing, is usually the first step applied during the image processing of radiographic images. The aim of this step is to reduce the random noise in the image without introducing systematic or non-linear deviations from the original image, which could lead to introduction of image processing artefacts in the final processed image. The following advanced smoothing algorithms were developed and implemented: methods for correction of outlier pixels, fully selectable 3x3, 5x5, and 7x7 convolution filters, polynomial 2D smoothing, fuzzy median smoothing, bilateral 2D smoothing, and adaptive local smoothing. Two-dimensional bilateral smoothing was identified as the most promising noise suppression method, because it takes into account both the closeness of the pixels (i.e., the filter includes coefficients that fall off with distance) and similarity of the pixels (i.e., the filter includes coefficients that decay with dissimilarity). The most important property of the bilateral smoothing filters is that they preserve edges, while other smoothing filters smear edges. The originally proposed bilateral 2D smoothing [2] used Gaussian functions for both spatial-domain coefficients and for grey-level coefficients. A generalized formula for bilateral filtering was proposed:

$$S_1(i,j) = \sum_{k=-M}^{M} \sum_{m=-M}^{M} A(i+k, j+m) \cdot Y(i+k, j+m)$$

where ***Y(i, j)*** represents the original image, ***S(i, j)*** represents the smoothed image, ***A(i+k, j+m)*** are the weights/coefficients of the bilateral 2D smoothing operator. In the formulae below, $\boldsymbol{\mu}$ and $\boldsymbol{\sigma}$ are the average and the standard deviation over pre-defined number of pixels, $\boldsymbol{\alpha_1}$ and $\boldsymbol{\alpha_2}$ are the multiplication coefficients, and ***M*** and ***N*** (***N<M)*** are the filter width/region and a sub-set of the filter region. Several functions for bilateral 2D smoothing operator were implemented and tested:

$$A(i+k, j+m) = e^{-\alpha_1 \cdot \left(\frac{|\mu_N(i,j)-\mu_M(i,j)|}{\sigma_M(i,j)+\sigma_N(i,j)} \right) \cdot (k^2+m^2)} \cdot e^{-\alpha_2 \frac{|Y(i+k,j+m)-\mu_N(i,j)|}{\sigma_N(i,j)} \cdot \frac{|Y(i+k,j+m)-Y(i,j)|}{|\mu_N(i,j)-\mu_M(i,j)|}} \tag{1}$$

$$A(i+k, j+m) = e^{-\alpha_1 \cdot \left(\frac{\sigma_M(i,j)}{\sigma_N(i,j)} \right) \cdot \left(\frac{|\mu_N(i,j)-\mu_M(i,j)|}{\sigma_N(i,j)+\sigma_M(i,j)} \right) \cdot (k^2+m^2)} \cdot e^{-\alpha_2 \cdot \frac{|Y(i+k,j+m)-Y(i,j)|}{|\mu_N(i,j)-\mu_M(i,j)|}} \tag{2}$$

$$A(i+k, j+m) = e^{-\alpha_1 \cdot \left(\frac{\sigma_M(i,j)}{\sigma_N(i,j)} \right) \cdot \left(\frac{|\mu_N(i,j)-\mu_M(i,j)|}{\sigma_N(i,j)+\sigma_M(i,j)} \right) \cdot (k^2+m^2)} \cdot e^{-\alpha_2 \cdot \frac{|Y(i+k,j+m)-Y(i,j)|}{|Y(i+k,j+m)-\mu_N(i,j)|}} \tag{3}$$

$$A(i+k, j+m) = e^{-\alpha_1 \cdot \left(\frac{\sigma_M(i,j)}{\sigma_N(i,j)} \right) \cdot \left(\frac{|\mu_N(i,j)-\mu_M(i,j)|}{\sigma_N(i,j)+\sigma_M(i,j)} \right) \cdot (k^2+m^2)} \cdot e^{-\alpha_2 \cdot \frac{|\mu_N(i,j)-\mu_M(i,j)|}{\sigma_M(i,j)} \cdot \frac{|Y(i+k,j+m)-Y(i,j)|}{|Y(i+k,j+m)-\mu_N(i,j)|}} \tag{4}$$

$$A(i+k, j+m) = e^{-\frac{|\mu_N(i,j)-\mu_M(i,j)|}{\sigma_M(i,j)} \cdot \frac{|Y(i+k,j+m)-\mu_N(i,j)|}{\sigma_N(i,j)} \cdot \frac{(k^2+m^2)}{\sigma_2}} \tag{5}$$

$$A(i+k, j+m) = e^{-\frac{|Y(i+k,j+m)-\mu_N(i,j)|}{\sigma_N(i,j).\sigma_M(i,j)} \cdot \frac{(k^2+m^2)}{\sigma_2}} \tag{6}$$

$$A(i+k, j+m) = e^{-\left(\alpha_1 \cdot \frac{|Y(i+k,j+m)-Y(i,j)|}{\sigma_M^2(i,j)} + \frac{(k^2+m^2)}{.\sigma_2^2} \right)} \tag{7}$$

$$A(i+k, j+m) = \frac{1}{\left(1 + \frac{[Y(i+k,j+m)-Y(i,j)]^2}{\sigma_1^2} \right)} \cdot \frac{1}{\left(1 + \frac{(k^2+m^2)}{\sigma_2^2} \right)} \tag{8}$$

$$A(i+k,j+m)=\frac{1}{\left(1+\frac{[Y(i+k,j+m)-Y(i,j)]^2}{\sigma_1^2}\right)}+\frac{1}{\left(1+\frac{(k^2+m^2)}{\sigma_2^2}\right)} \tag{9}$$

$$A(i+k,j+m)=\frac{1}{\left(1+\frac{|Y(i+k,j+m)-Y(i,j)|}{\sigma_N(i,j)+\sigma_M(i,j)}\right)}\cdot\frac{1}{\left(1+\frac{(k^2+m^2)}{\sigma_2^2}\right)} \tag{10}$$

$$A(i+k,j+m)=\frac{1}{\left(1+\alpha_1\cdot\frac{[Y(i+k,j+m)-\mu_N(i,j)]^2}{\sigma_N(i,j).\sigma_M(i,j)}\right)}\cdot\frac{1}{\left(1+\frac{(k^2+m^2)}{\sigma_2}\right)} \tag{11}$$

$$A(i+k,j+m)=\frac{1}{\left(1+\frac{[Y(i+k,j+m)-\mu_N(i,j)]^2}{\sigma_1^2}\right)}+\frac{1}{\left(1+\frac{(k^2+m^2)}{\sigma_2^2}\right)} \tag{12}$$

All of the above functions differ from the original formula for the coefficients for bilateral smoothing, see Equation (13).

$$A(i+k,j+m)=e^{-\left(\frac{|Y(i+k,j+m)-Y(i,j)|}{\sigma_1}+\frac{(k^2+m^2)}{\sigma_2^2}\right)} \tag{13}$$

The original image and two processed images are shown in Figure 2 and their operators noted in the caption. Results from the comparison of different implementations of the bilateral 2D smoothing operators are shown in Table 1. The area shown in red in Figure 2(a) was used to calculate the signal-to-noise ratio (SNR). The presented images are in 8-bit JPG format, while the original were bigger images (512x512 pixels) in 16-bit TIF format, so it is not possible to correctly evaluate the spatial resolution from the images presented herein. As can be seen from Table 1, only Equations (2), (3) and (10) preserve the spatial resolution as per the original image, with Equations (2) and (10) achieving the same improvements in SNR as a 7x7 Gaussian filter. The original bilateral smoothing [2] and Equation (8) achieve better SNR and better spatial resolution than polynomial smoothing. Equations (9) and (12) achieve better SNR and better spatial resolution than polynomial 5x5 averaging. It should be noted that the results presented in Table 1 are for specific values of the parameters for each filter, and different selection of parameters will lead to different results. Optimization of the parameters of the proposed bilateral 2D smoothing operators was outside the scope of the current research.

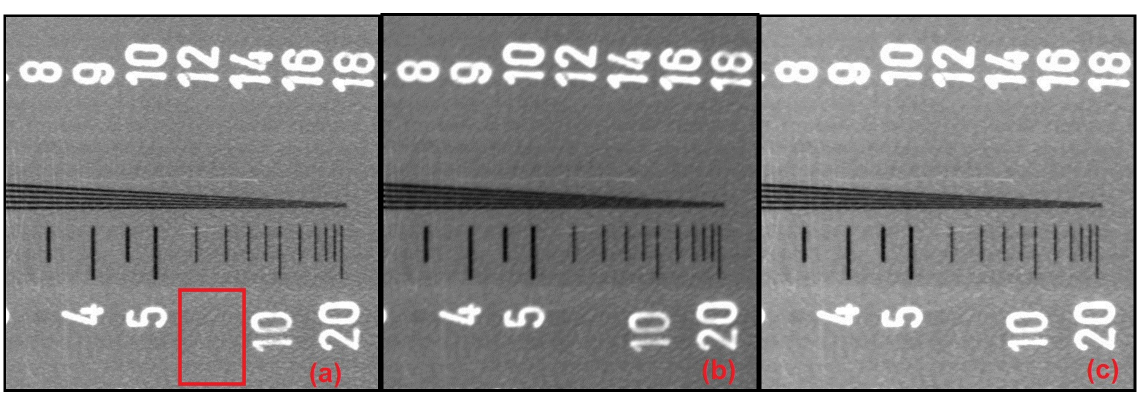

Figure 2. Examples of smoothing operators: (a) original image, (b) polynomial smoothing, and (c) bilateral smoothing using Eq. (9).

Table 1. Comparison of SNR and LP (Line-Pairs) of different smoothing algorithms.

Image	SNR	Spatial Resolution [LP/mm]	Filter Parameters
Original	17.4	9	
Selectable Filter 5x5 (Average)	30.7	4.5	
Selectable Filter 7x7 (Gaussian)	25.1	7	
Polynomial Smoothing	27.1	6	F1, 2, 2
Original Bilateral Smoothing	29.3	8	3, 3, 0.05
New Bilateral Smoothing Eq. (1)	23.7	8	1, 0.1, 3, 0.1
New Bilateral Smoothing Eq. (2)	25.1	9	1, 0.1, 3, 0.4
New Bilateral Smoothing Eq. (3)	22.6	9	1, 0.2, 3, 1
New Bilateral Smoothing Eq. (4)	19.0	8	1, 0.2, 3, 0.5
New Bilateral Smoothing Eq. (5)	19.0	7	1, 3, 1
New Bilateral Smoothing Eq. (6)	18.5	8	1, 3, 0.001
New Bilateral Smoothing Eq. (7)	21.8	8	1, 2, 1
New Bilateral Smoothing Eq. (8)	27.3	8	3000, 3, 1
New Bilateral Smoothing Eq. (9)	33.6	6	3000, 3, 1
New Bilateral Smoothing Eq. (10)	25.1	9	1, 3, 2
New Bilateral Smoothing Eq. (11)	22.6	8	1, 0.1, 3, 3
New Bilateral Smoothing Eq. (12)	34.5	5.5	1, 3000, 3, 1

Additionally, formulae and an algorithm for a 2D smoothed derivatives calculation was developed. Results from applying this algorithm are presented in Figure 3. The smoothed derivatives operation combines noise suppression with visibility enhancement, and can be useful for simultaneous observation of objects with different thickness in the radiographs. It should be noted that the original image looks darker in comparison to the case when viewed on professional radiography monitor, due to the limited contrast for images in PDF and Microsoft Office files. Nevertheless, the improvements demonstrated in this presentation cannot be achieved with simple intensity and brightness adjustments of the original image.

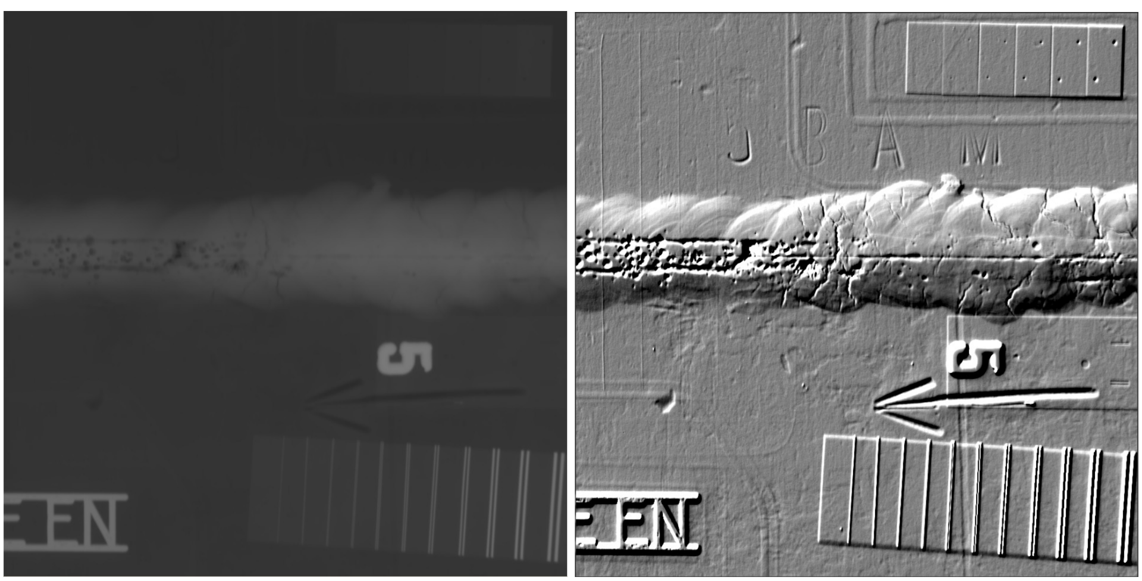

Figure 3. Original image (on the left) and smoothed 2D derivative (on the right).

2.2 Contrast enhancement methods

Contrast enhancement methods are used for improvement of the visibility of details in digital radiographs. Contrast enhancement allows for simultaneous visualization and observation of defects and internal parts which could not be viewed simultaneously in the original image, for example details and/or defects located in parts of the object which have a significant difference in thickness. The wide range of thickness variation will lead to a very wide range in grey-scales in the radiographic image. The human eye can distinguish only about 32 different grey-levels, so it will be impossible to observe internal details in the radiographic image without application of appropriate image enhancement techniques. It is important to visualise and observe simultaneously the whole thickness range recorded in the radiographs in order to perform proper diagnostics and interpretation. This requires strong image enhancement algorithms and advanced visualization methods. Several different types of algorithms for contrast enhancement were developed and implemented:

- Sharpening filters (17 sharpening filters with selectable parameters were implemented),
- Local contrast enhancement algorithms,
- Adaptive unsharp mask algorithms,
- Adaptive contrast enhancement,
- Contrast enhancement by digital equalization (CEDE).

Examples of image contrast enhancement methods are presented in Figure 4.

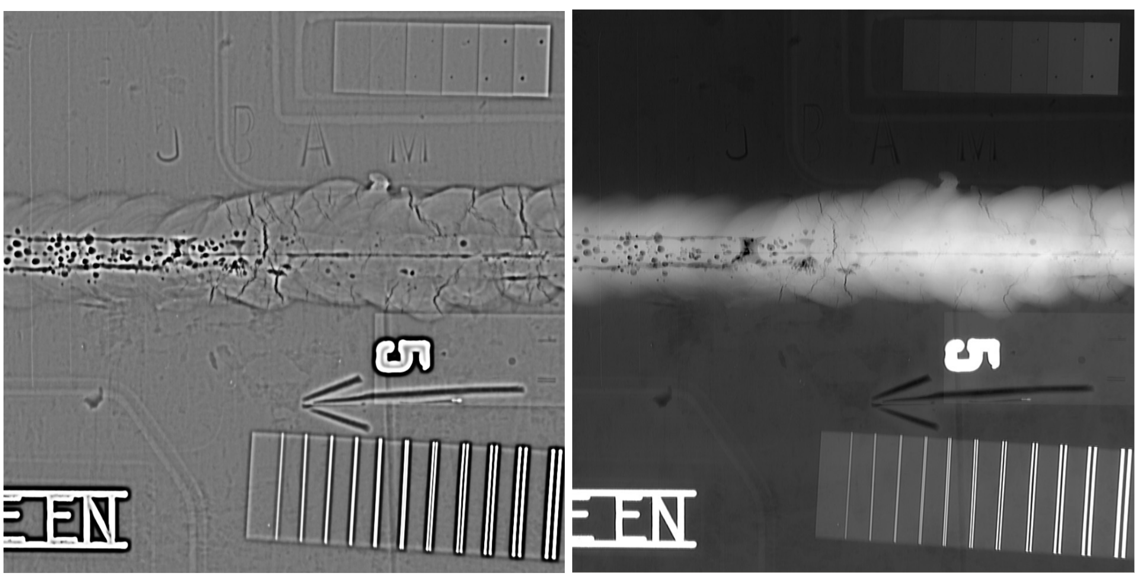

Figure 4. CEDE (left), and local contrast enhancement (right). Original image is in Figure 3.

2.3 Grey-scale manipulation methods

Most of these algorithms are based on global or localized histogram equalization, or on other advanced methods like differential hysteresis filtering. Some of the developed and implemented algorithms are:

- Sigmoidal intensity adjustment with multiple types of functions,
- Auto sigmoidal intensity adjustment,
- Auto gamma histogram equalization,
- Local histogram equalization,
- Contrast limiting adaptive histogram equalization (CLAHE),

- Random sampling local histogram equalization (RSLHE),
- Local intensity stretching with bi-linear interpolation (LISBLI),
- Local intensity rank filtering.

Several examples of images processed with grey-scale manipulation methods are presented in Figure 5.

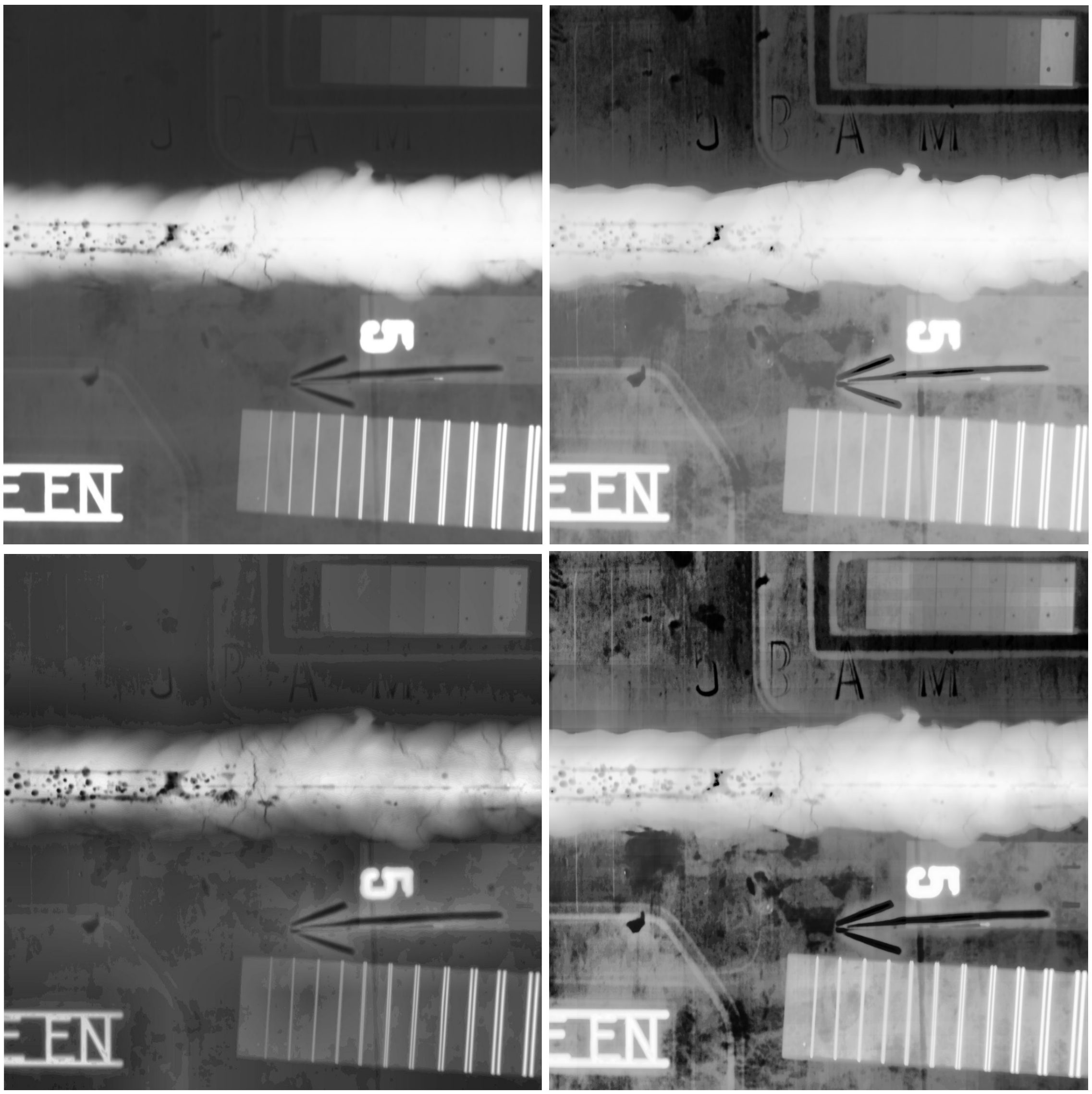

Figure 5. Auto sigmoidal intensity adjustment (left top), auto gamma histogram equalization (right top), CLAHE (left bottom), and RSLHE (right bottom). Original image is in Figure 3.

2.4 Statistical image analysis methods

Image processing methods, based on calculation of different local statistical parameters, were developed and implemented. Some of the implemented algorithms are based on the following local statistical quantities: signal variance, entropy, adaptive histogram entropy, signal-to-noise ratio, contrast-to-noise ratio, etc. Examples of statistical methods are shown in Figure 6.

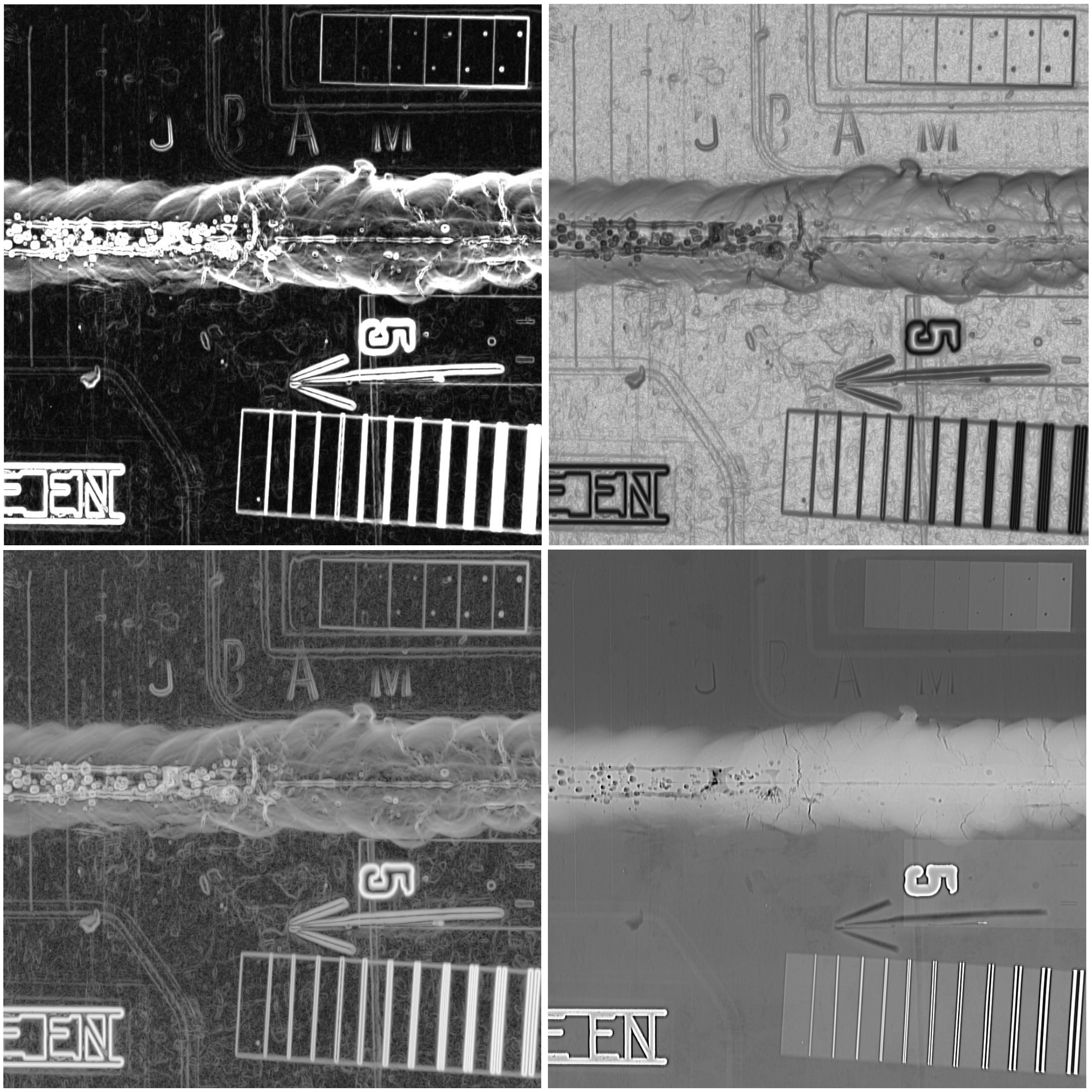

Figure 6. Image processing methods based on local signal variance (left top), local SNR (right top), logarithmic signal variance (left bottom), and local entropy (right bottom). Original image is in Figure 3.

2.5 FFT based methods

The Fourier transform is widely used in different fields of science. It is based on two basic functions: sine and cosine. These functions have infinite range in the space domain, but they are completely localized (δ-functions) in the frequency domain. Because of the choice of the basic functions, Fourier analysis is very well suited for studying periodic signals. In other words, Fourier analysis is not local in space, but is local in frequency. The most widely used digital implementation of the Fourier analysis is the Fast Fourier Transform (FFT), which allows for fast transformation/computation when the number of the points is 2^N, where N is an integer number > 3. The signal filtering is done in the frequency domain, usually by applying a bandpass filter, which can lead to simultaneous reduction of the random noise and enhancement of details visibility. An example of FFT-based image processing is presented in Figure 7.

2.6 DWT based methods

The wavelet transform maps the input data into a new space, the basic functions of which are quite localized both in the space domain and in the frequency domain. The term “wavelet” means “small wave” and represents a localized wave-like function. Wavelets are localized in frequency as well as space, i.e. their rate of variation is restricted in both domains, which make them very suitable for analysing fast-changing (in time or space) signals. While the Fourier analysis is unique (i.e., there are only two basic functions: sine and cosine), the wavelet analysis is not unique, and there are many possible sets of wavelets which one can use. The trade-off between different wavelet sets is between their compactness versus their smoothness. Another advantage of the wavelet transform is that it is less computationally complex (i.e., it is faster than the Fast Fourier Transform). The discrete wavelet transform (DWT) is implemented by means of filter banks. The input signal has been split into frequency bands, by means of application of low-pass and high-pass filters. The DWT is usually implemented using a pyramidal algorithm, and at the end we have two sets of coefficients: details coefficients for all decomposition levels, and the approximation coefficients for the last level.

Two types of filtering of the input image were developed using DWT: a low-pass filter (or convolution with a smoothing function) and a high-pass filter (or convolution with a differentiating function). The following DWT image smoothing operators were implemented in the software: hard threshold, soft threshold, affine threshold, Garrote threshold, and smoothly clipped absolute deviations (SCAD) threshold. The following DWT image enhancement operators were implemented in the software: phase only reconstruction, piecewise linear function, gamma function, log function, Stahl Function, and gamma-sigmoidal function. In addition, several combined smoothing and enhancement DWT operators were implemented, based on sigmoidal, power, and exp-gamma functions. All of the above described operators use the same filter function for all details coefficients of all decomposition levels and for the approximation coefficients for the last level. Separately, two multi-scale enhancement algorithms were developed and implemented, based on application of a different filter/enhancement function for details coefficients of each different decomposition level. An example of DWT image processing is presented in Figure 7.

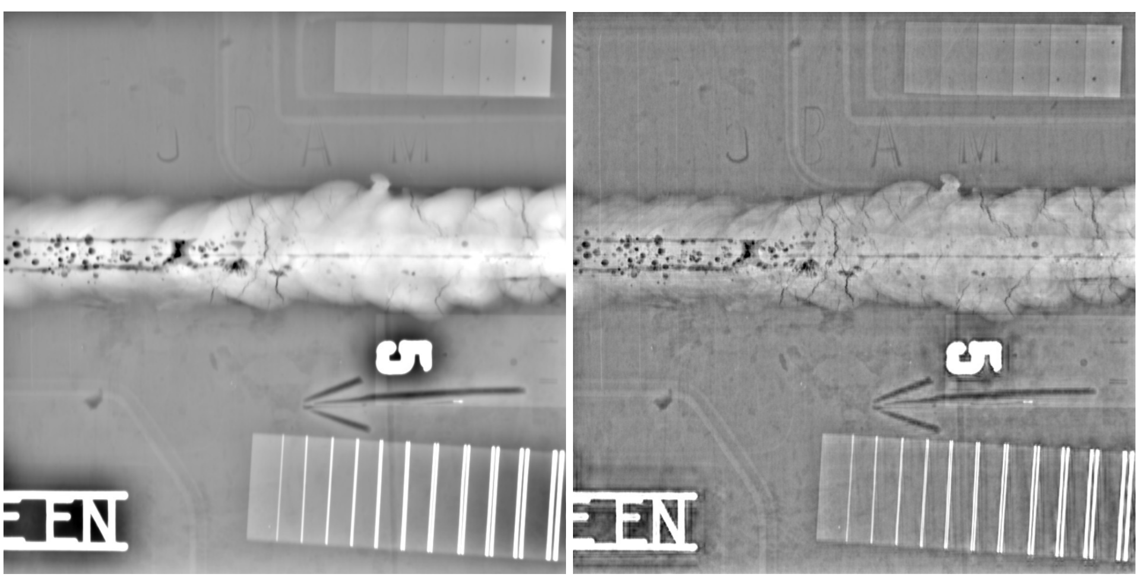

Figure 7. FFT band-pass filtering (left), and multi-level DWT based image processing (right). Original image is in Figure 3.

3. Conclusions

Digital radiography is significantly faster and offers improved detection latitude and better contrast, sensitivity and SNR in comparison to classical film radiography, which could lead to financial advantage during inspections. Advanced image processing can bring noticeable improvement in the visibility and detection of details in the radiographic images. CNL has developed prototype image processing software, to be used for implementation and testing of new image processing algorithms. At the current stage, all basic editing and image manipulation functions are implemented, together with some advanced image processing algorithms, which belong to three groups: noise suppression, contrast enhancement, and grey-scale manipulation for visibility improvement. Examples of the developed and implemented algorithms include polynomial and adaptive smoothing, statistical image evaluation tools, adaptive contrast enhancement, non-linear histogram adjustment algorithms, FFT and DWT image enhancement methods, etc. The developed software platforms can be used for further research work in the field of radiography image processing, and for the development and testing of new image processing algorithms. Development of advanced image processing methods would be beneficial not only to digital radiography, but to all other image-producing NDT methods, such as visual inspection (digital cameras are used on a regular basis for collecting data during visual inspections, and can greatly enhance the productivity of such methods as liquid penetrant and magnetic particles testing), ultrasound imaging, etc.

It should be noted that image processing can introduce artefacts into the images, and in this respect, the image processing software should be considered only as an aid during the interpretation and flaw-sizing of the digital radiographic images. Any indication detected in the enhanced radiograph should be confirmed with simple intensity stretching (this is equivalent to changing the intensity of the radiographic film viewer), as per the ASME code requirements [3]. Only indications that are confirmed in this way should be reported.

It would be useful for the radiographic community to generate several standardized digital radiography images (for example, images of welds and castings), which can be used to formalize and standardize the requirements and methods for testing radiographic image processing methods and software. The path forward is to organize a round-robin test for comparing capabilities of currently available image processing programs and for evaluating new image processing algorithms. Quantification of the capabilities of the image processing algorithms is needed in several areas, such as noise suppression, SNR improvement, minimum observable flaw or Image-Quality-Indicators feature in enhanced images, and evaluation of artefacts introduced by the image processing methods.

References

1. K. Stoev, "Comparison of Radiographic Image Processing Algorithms", Proceedings of 6th European Workshop on Structural Health Monitoring, v.2, p. 1639 (P29), July 2-6, 2012, Dresden, Germany (http://www.ecphm2012.com/Portals/98/BB/p29.pdf).
2. C. Tomasi and R. Manduchi, "Bilateral Filtering for Gray and Color Images", Proceedings of the 1998 IEEE International Conference on Computer Vision, Bombay, India, 1998.
3. ASME Boiler and Pressure Vessel Code, Section V "Nondestructive Examination", Article 2 "Radiographic Examination", Mandatory Appendix IV "Interpretation, Evaluation, and Disposition of Radiographic and Radioscopic Examination Test Results Produced by the Digital Image Acquisition and Display Process", 2010 edition.